Intrinsic elastic properties of Calcium Silicate Hydrates by nanoindentation

C. Plassard, E. Lesniewska, I. Pochard, A. Nonat
University of Bourgogne, Dijon, France

Abstract

Calcium Silicate Hydrate (C-S-H) nanoparticles were partially recrystallized by Ostwald ripening after long-term equilibrium in calcium hydroxide solution of different concentration, leading to C-S-H of different Ca/Si ratio. The atomically smooth microdomains obtained have made possible the investigation of the intrinsic elastic properties of C-S-H in the direction perpendicular to the plane of the silicate layers. This has been carried out by nanoindentation using an experimental device based on the Atomic Force Microscope. Results have shown that the intrinsic elastic modulus of C-S-H drastically increases with the Ca/Si ratio, which may be explained by the change in structural and chemical properties of the C-S-H interlayer. Results for C-S-H of low Ca/Si ratio are in perfect agreement with theoretical results of the literature. It is, to our knowledge, the first time that experimental values of the intrinsic elastic modulus of C-S-H particles are reported. It could bring some important insight to the understanding of mechanical properties of cement-based materials.

1. Introduction

Understanding the mechanical properties of concrete is one of the main purpose of the science of cement [1,2]. This is not a straightforward question as concrete is a complex heterogeneous material and its properties depend on its microstructure, *i.e.* the volume fraction and the properties of the different phases. One may believe that if the specific properties of all phases are known, the effective properties of the composite material can be predicted. Simple and complex models based on micro-mechanical properties of the individual phases constituted the bulk matrix of hydrated Portland cement have been applied to explain or predict the behaviour of cement-based materials [3-7]. The phase properties and volume fractions have been used in a model that predicts the macroscopic elastic properties of cement pastes [8]. Haecker *et al* [9] have described a finite element procedure based on knowledge of individual phase moduli and cement paste microstructure model to quantitatively predict elastic moduli of cement pastes.
Lots of works report results on nanoindentation of composite materials or thin films [10-15] and great efforts have been undertaken to link properties of sintered materials to their porosity. The question arising is: is it possible

to measure intrinsic mechanical properties of material by nanoindentation measurements on porous samples? Only Surface Force Microscopy is able to carry out indentation at a nanoscopic scale and the works reporting nanoindentation in literature are scarce [10]. Actually, the characteristic length of the indentation area on porous samples is on the order of 10^{-6} m [16] and is therefore much dependent on porosity. Attempts have been carried out to extract intrinsic material properties from indentation experiments on porous materials, like by finite element analyses and by taking into account substrate and densification effects [17]. This approach gives in fact intrinsic properties of the porous film but not of the material itself. In most cases, intrinsic values are obtained by extrapolation back to zero porosity [6,7,18,19]. But this method is much dependent on the chosen model for calculation of the intrinsic data and is generally not satisfactory.

Little is known about the mechanical contribution of C-S-H nanoparticles on the mechanical properties of cement-based materials. Such data are, however, important as C-S-H phase dominates the volumetric proportions of cement paste materials, and its contribution to the macroscopic mechanical performance is therefore significant. But not being able to handle C-S-H crystals, we are not able to measure the bulk mechanical properties by traditional techniques (oscillation, flexion). However, Atomic Force Microscopy allows measurement of the elastic modulus of nanomaterials by indentation at nanoscale [20-22].

Atomic Force Microscopy already contributed significant input in this area and especially in the measurement of the interaction forces between C-S-H particle surfaces [23-26] and in the imaging of the growth of C-S-H [27]. The formation of C-S-H on flat surfaces has been studied by Atomic Force Microscopy (AFM) in each case, on alite, silica glass and calcite surface. In all cases, C-S-H precipitates on the surface by first forming an orientated aggregation of identical thin nanoparticles, the plane of the layers being parallel to the plane of the substrate [26,28,29]. In the case of the C-S-H coverage onto calcite, for which the substrate does not react in the equilibrium solution of C-S-H, a long equilibrium time allowed partial recrystallization. So, micrometric atomically smooth domains were revealed. On such atomically plane area, atomic resolution rendered possible investigation of the C-S-H surface structure. It has been then possible to measure the evolution of the surface cell parameters and the silicate chain length versus the Ca/Si ratio of the solid [27]. In connection with the indentation depth on these atomically flat areas, the mechanical properties of the C-S-H crystals have been probed. Nanoindentation leads to the intrinsic elastic modulus of the C-S-H material in the direction perpendicular to the plane of the layers.

After checking the method with materials of known Young modulus, results on C-S-H single crystals are presented. All these results will be discussed and compared to theoretical and experimental works of the literature.

2. Materials and methods

2.1 Experimental set-up

All experiments were performed into a glove box free from carbon dioxide to prevent carbonation of hydroxide solutions. Inside, a multimode atomic force microscope (AFM) (Nanoscope IIIa; Veeco Co., CA) equipped with different scanners (0.8 – 150 µm) was operated in contact mode. The microscope was kept at over 80% relative humidity under a glass bell-jar by passing a decarbonated flux of dry nitrogen gas through calcium hydroxide solution. For studies in aqueous solutions, an adapted commercial fluid cell associated with a fluid exchange system was used to maintain steady bulk concentrations for all diffusion processes acting on the C-S-H crystal. Equilibrated prepared calcium hydroxide solutions flowed through the fluid cell. The temperature of the surrounding wall was maintained at 25°C. We have used rectangular stainless steel cantilevers (DNISP nanoindentation probe; Veeco Co., CA) associated to a diamond probe with a radius of curvature at the apex of about 25 nm. The cantilever spring constant was about 210 N/m, measured by resonance frequency method (64 kHz, sensitivity 176 nm/V used for spring constant calibration). The typical depth of the indentation was less than 10 nm. The stiffness of C-S-H substrate was at least 20 times larger than the depth of indentation. The elastic modulus of calcite $CaCO_3$ crystal (Iceland spar) was measured perpendicularly to the {10$\bar{1}$4} cleavage calcite plane equal to 75±3 GPa, in agreement with literature [30].

2.2 Substrate preparation

C-S-H coverage was obtained by immersion of a single crystal of calcite in a concentrated sodium silicate solution (pH=14.2). The following chemical reaction occurs:

$$CaCO_3 \rightarrow Ca^{2+} + CO_3^{2-} \qquad (1)$$

$$xCa^{2+} + 2(x-1)OH^- + H_2SiO_4^{2-} \rightarrow (CaO)_x - (SiO_2) - (H_2O)_y \qquad (2)$$

Silicate concentration was chosen in such a way to shift equilibrium to C-S-H precipitation. C-S-H precipitates on the calcite surface in the form of identical nanoparticles (60x30x5 nm^3). To obtain a sufficient coverage of C-S-H, the reaction between the calcite and the sodium silicate solution must continue for about one week. Then, the C-S-H covered single calcite crystals are immersed in different calcium hydroxide solutions ($0.16<[Ca(OH)_2]<19.13$ mmol/L) for one month to obtain C-S-H of different stoichiometries. The thickness of the C-S-H layer was in the range 200-700 nm depending on the calcium hydroxide concentration (increasing with the calcium hydroxide concentration increase). There was no dependence of the calcite substrate on nanoindentation measurement. At least, 5 different C-S-H crystals for each of the 8 different concentrations

were thus analyzed: 0.16 mmol/L, 0.82 mmol/L, 1.84 mmol/L, 3.15 mmol/L, 4.53 mmol/L, 10.31 mmol/L, 14.69 mmol/L, 19.13 mmol/L. For comprehensive clarity, we labelled each set of C-S-H crystal sample 1 to 8. The advantages of single calcite crystals are two-fold: the initial surface is atomically smooth and its surface is non-reactive when the sample is in contact with the different calcium hydroxide solutions which provide different C-S-H stoichiometries. After one month of equilibration in the calcium hydroxide solutions, micrometric atomically smooth domains appeared (Fig. 1). It must be mentioned that C-S-H nanoparticles are still present in the lowest part of the sample. These atomically smooth microdomains made possible the investigation of the intrinsic elastic properties of the C-S-H material in the direction perpendicular to the plane of the layers by mean of nanoindentation.

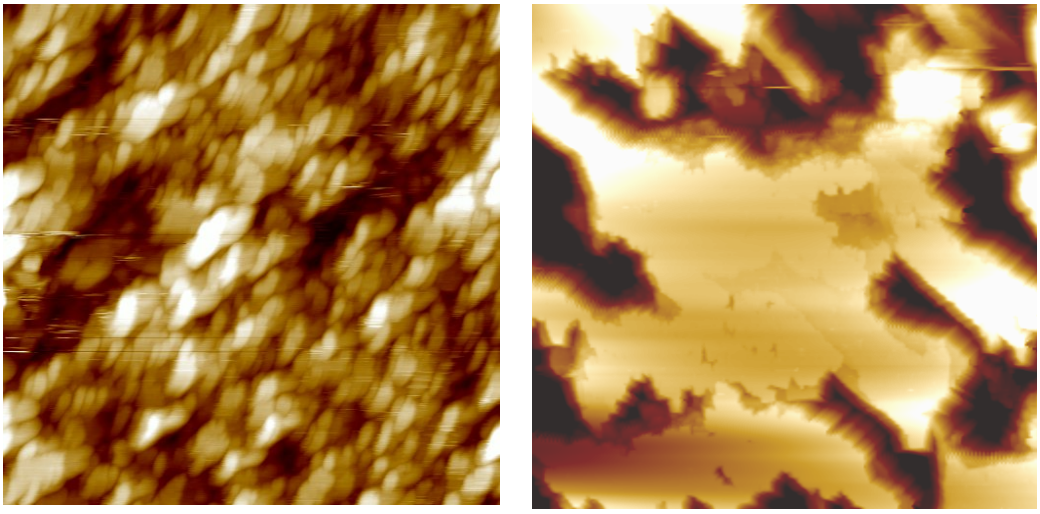

Figure 1. Atomic Force Microscopic image of C-S-H obtained on a calcite single crystal. (left) C-S-H nanoparticles at the start of equilibrium in calcium hydroxide solution. 1x1 µm² image. (right) C-S-H atomically smooth domains after one month equilibrium in calcium hydroxyde solution. 5x5 µm² image. Relative height: 200 nm.

2.3 Nanoindentation

An experimental device based on the Atomic Force Microscope has been adapted allowing the application of normal force at the sample surface by compensating the inclination of the AFM cantilever of about 12°. By choosing cantilevers with higher stiffness constant, it is possible to account for evolution of mechanical properties of nanomaterials with nanoindentation, we can follow the evolution of the force *F* corresponding to the indentation appliedδ; which differed according to the nature of the material. The studied C-S-H samples showed behaviour similar to that of mixed materials.

For calibration, load frame compliance was performed by pushing AFM probe on a smooth sapphire sample. In this case, because the sample contact stiffness is much higher than the probe spring constant, no tip penetration occurs and the measured force-displacement response is characteristic of the given AFM probe. The probe response can be subtracted from the force-displacement responses measured on the C-S-H samples so that only the force-displacement response remains.

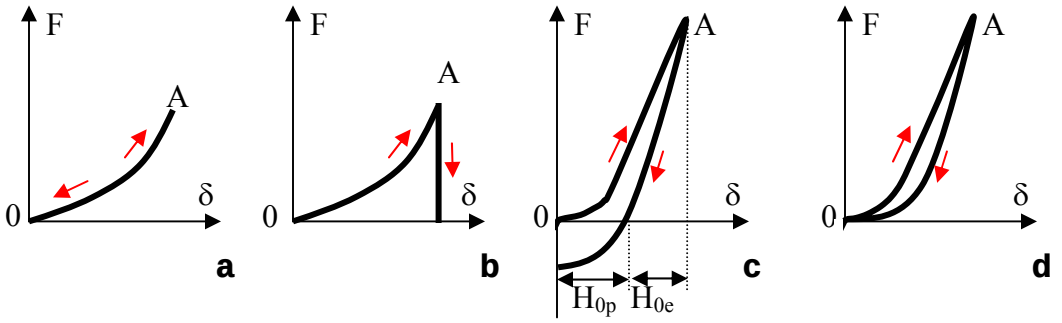

Figure 2. Stress (*F*) versus indentation (δ) characteristic. (a) Ideal elastic behaviour (pure elastic material). (b) Plastic elastic behaviour (pure plastic material). (c) Intermediate elastic-plastic behaviour (mixed material) with adhesion. H_{0p} and H_{0e} represent the plastic part and the elastic part for zero load respectively; (d) Pure elastic-plastic behaviour.

Eight load levels ranging from 100 pN to 10 nN were used to indent the C-S-H samples. For each load level, ten force curves were obtained on sapphire before and after indenting C-S-H sample, using the same probe and operating conditions. Smooth spline curves were fit to the unloading curves after successful attempts to get good fits using nonlinear power law fits and linear fits to logarithmic data.

To reach the elastic modulus, it was necessary to compare the results of various theories. By using two basic theories [31] considering the probe as a sphere, these emerges a good interpretation. The amplified model of Hertz does not take into account the adhesion between tip and surface and considers an elastic sphere of radius R faces a rigid plan (C-S-H crystal):

$$E = 3\left(1-\nu^2\right)k\,\Delta z/\left(4\,\delta^{3/2}R^{1/2}\right) \quad (3)$$

with ν being Poisson's ratio of the diamond probe, k the stiffness constant of AFM cantilever, Δz the displacement of the piezoelectric scanner and δ the indentation. The Mathlab program fits the indentation, the slope of the elastic contribution, and calculates the displacement of the piezoelectric scanner, and the adhesion force.

The other model used is the JKRS (Johnson Kendall Roberts Sperling) model, which neglects the long range forces outside the contact area and considers only the short range force inside the contact area:

$$E = 0{,}65\,k\,\Delta z - 3{,}28\,R^{3/4}k^{1/4}\Delta z^{1/4}F_{adh}^{3/4}/\left(\delta^{3/2}R^{1/2}\right) \quad (4)$$

with F_{adh} being the adhesion force between tip and sample surface.

3. Results and discussion

3.1 Validation of the experimental method

As the indentation procedure has been adapted from an experimental device based on the Atomic Force Microscope, it was nonetheless necessary to first validate the experimental method on material of known mechanical properties. This was done on foshagite $Ca_4Si_3O_9(OH)_2$ and muscovite green mica.
The foshagite, studied by X-Ray Diffraction [32], presents a monoclinic unit cell with lattice parameters: *a=10.32 Å, b=7.36 Å, c=7.04 Å, β=106.4°*. The DFT calculations of the elastic modulus in the (010) direction give E_{calc}*=190 GPa* [33]. In experiments, the (010) plane of foshagite was indented in about twenty different areas with five measurements per area. The elastic modulus was then calculated by the Hertz and JKRS theories, and the average following results were obtained: E_{Hertz}*=193±26 GPa* and E_{JKRS}*=184±22 GPa.* These experimental results are in close agreement with the calculated modulus of E_{calc}*=190 GPa.*
The same control experiment was performed on the freshly cleaved (001) face of the muscovite green mica. The elastic modulus along the *c-axis* was estimated after ten indentations. The values were: E_{Hertz}*=49.9±1.5 GPa* and E_{JKRS}*=46.2±1.4 GPa*. The elastic modulus measured by Vickers indentation was 48 GPa along the *c-axis* [34].
These two experiments allow to validate the procedure for elastic modulus values from few tens GPa to few hundreds GPa. We could thus plan to reproduce these indentations on the C-S-H crystals.

3.2 Nanoindentation on C-S-H substrates

For each samples, the elastic modulus was averaged from results obtained by both Hertz and JKRS theories on hundred measurements. Eight samples were analyzed after equilibrium with calcium hydroxide solutions of different concentration (see § 2.2). The evolution of the elastic modulus according to the calcium hydroxide concentration present in the equilibrium solution is depicted in Fig. 3. Different behaviors between samples 1 to 5 and 6 to 8 can be noticed: A fast evolution of the elastic modulus is observed up to a concentration of 4.53 mmol/L; then, an inflection occurs for a concentration of about 8 mmol/L and a quasi stability of the elastic modulus takes place for the higher concentrations. Within the increase in calcium hydroxide concentration from almost zero to 20 mmol/L, the intrinsic elastic modulus of C-S-H parallel to the direction of the layers has been multiplied by almost ten.
This evolution of the elastic modulus may be related to the structural characteristics of the interlayer of C-S-H. For the lowest calcium hydroxide

concentration, binding bounds of silicate tetrahedra are essentially silanol groups: the cohesion between the layers is due to silanol-water-silanol (-OSiOH-H_2O-HOSiO-) bonds. By increasing the calcium hydroxide equilibrium concentration, we expected a modification in the nature of the chemical bond. Indeed, silanol groups are increasingly ionized as the calcium hydroxide concentration increases and the negative charges created are balanced by Ca^{2+} ions in interlayer. The (-OSiOH-H_2O-HOSiO-) bonds are therefore replaced by an iono-covalant -SiO--Ca^{2+}--SiO- bond, causing a reduction in the interlayer space *c* between two calcium planes. In consequence, the compactness of C-S-H crystal cell increases and the elastic modulus rises by a factor ten.

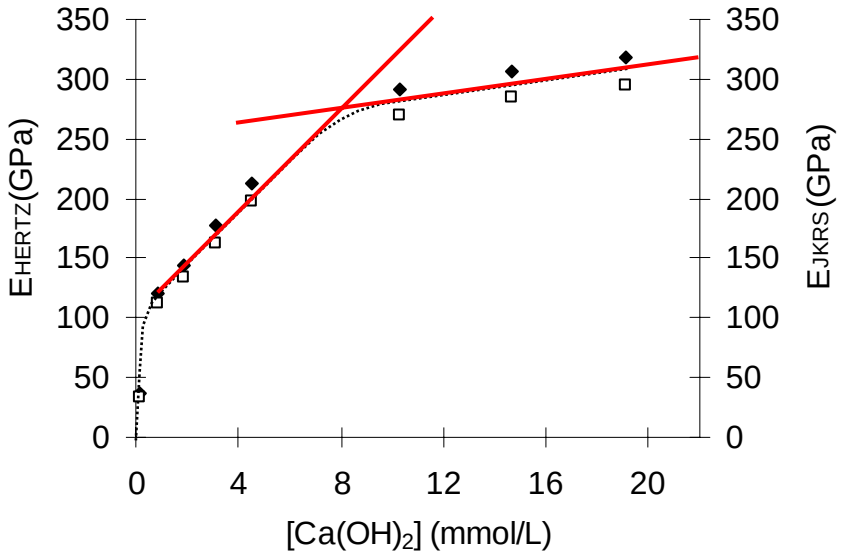

Figure 3. Variation of the intrinsic elastic modulus of C-S-H parallel to the direction of the layers versus the calcium hydroxide concentration in equilibrium solution. Results obtained by both Hertz and JKRS theories are presented. We report extrapolations for the linear ranges between 1 and 6 mmmol/L and between 11 and 19 mmol/L.

In addition, it has been shown, in the literature that the distance *c* between two Ca^{2+} planes as measured by X-ray diffraction declines sharply when the calcium hydroxide concentration increases (see Fig. 4) [35]. These observations are in perfect agreement with the results revealed by nanoindentation.

C-S-H at a concentration of about 1mmol/L could be compared to tobermorite. The elastic modulus of tobermorite was calculated [36]. The authors calculated the elastic modulus of a system based on independent tobermoritic layers (not chemically dependent). Only the deformations perpendicular to the interlayers were considered: the perpendicular elastic modulus was estimated equal to 81 Gpa, which is in good agreement with our experimental values. Unfortunately, no calculated data are available

for C-S-H in equilibrium with higher calcium hydroxide concentration. In this case, the values of C-S-H Young modulus are in the order of magnitude of values for silicon single crystal [37] or for ZrO_2-Y_2O_3 thin films [13].
The values of elastic modulus obtained in the present work are far from values reported in the literature for C-S-H in cement pastes, which are in the range 20-30 GPa [4,5,16,38,39]. But, one has to keep in mind that the present results and the one of Gmira *et al* [36] have been obtained for a single crystal of C-S-H whereas the whole references on mechanical properties of cement-based materials concern porous samples [4,5,8,16,38-41].

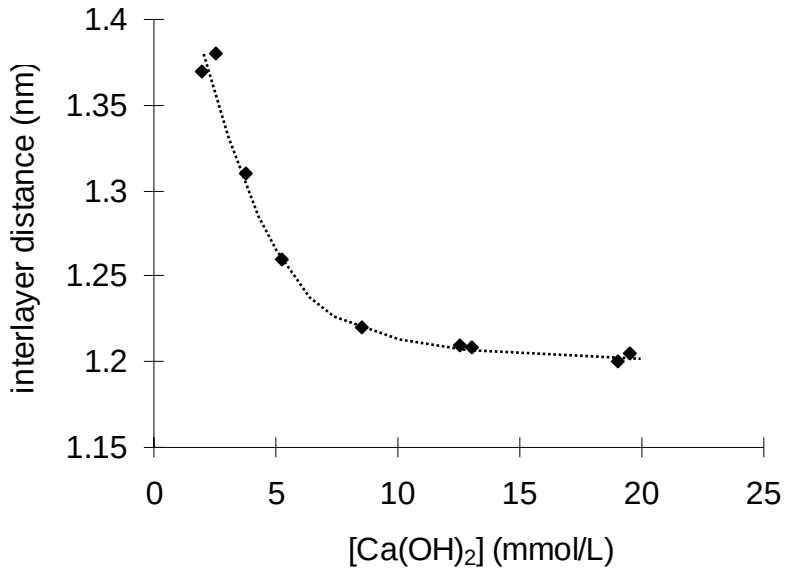

Figure 4. Variation of the C-S-H interlayer distance (measured by XRD) versus the calcium hydroxide concentration in the equilibrium solution. The line is only guide to eyes.

It is obvious that porosity is of main importance when measuring stiffness of materials. The values reported for Young modulus of the so-called Low Density LD (E = 21.7 GPa) and High Density HD (E = 29.4 Gpa) C-S-H as defined by the Tennis-Jennings model [42,43] enclose the C-S-H gel porosity [16]. Only the multiscale approach of the poroelastic properties of concrete developed by Ulm *et al* [41] reports values of elastic modulus of C-S-H at a lower scale (named “level 0” by the authors). This level, concerning the C-S-H basic building blocks or globules named by Jennings [43], is free from the gel porosity and thus presents a Young modulus much higher (47.75 GPa) than the ones of the LD and HD C-S-H. The C-S-H single crystal samples used in the present study could not be compare to Jennings model like no porosity was observed. The study was focused on the elastic properties of a single C-S-H nanoparticle not on the network of C-S-H nanoparticles corresponding to the basic units described

by Jennings [43], which explains the great values obtained for the Young modulus.

On C-S-H porous samples, only average stiffness values are accessible, including, as said before, the C-S-H gel porosity and eventually some fine calcium hydroxide crystals intimately mixed with the gel [8]. If neither the gel porosity nor the solid composition (Ca/Si ratio, calcium hydroxide inclusion) change then, the stiffness of the C-S-H phase remains the same for different cement-based materials [40]. But this becomes false if the material experiences porosity or composition modifications, which may occur in the case of calcium leaching for example.

Constantinides showed that calcium leaching leads to a loss of elastic stiffness [16]. The loss of C-S-H stiffness can be attributed to the decalcification of C-S-H and/or the increase of microporosity. Whereas Beaudoin and Feldman [44] provided experimental data of the mechanical properties of C-S-H with different Ca/Si ratios suggesting that the intrinsic elastic properties of C-S-H are independent of the Ca/Si ratio, Constantinides concludes the opposite showing the significance of C-S-H decalcification compared to the increase of microporosity on the overall loss of elastic stiffness. This result is in agreement with what we demonstrate here *i.e.,* that the elastic properties of C-S-H drop dramatically when the Ca/Si ratio decreases.

Conclusion

It has been possible to investigate the mechanical properties of C-S-H crystals supported by single calcite crystals with the aid of the atomic force microscope used as a nanoindenter. Elastic properties have been studied according to the direction perpendicular to the silicate layers. An increase in the calcium hydroxide concentration generates an increase in the value of the elastic modulus of C-S-H crystal. Indeed, a change in the nature of the chemical bonds is expected, causing a reduction in the interlayer space *c* between two layers. Values of elastic modulus show a discontinuity when the equilibrium concentration is about 8 mmol/L. This discontinuity may suggest a phase transition as has been suggested by other investigations [45,46].

To our knowledge, it is the first time that elastic properties of C-S-H nanoparticles are experimentally probed. The discrepancies observed between our own data and the values of elastic modulus of C-S-H in cement pastes are explained by the porosity. Actually, the present results have been obtained on a single crystal of C-S-H whereas the whole references on mechanical properties of cement-based materials concern porous samples.

The elastic modulus of a single crystal will give an anisotropic elastic moduli tensor reflecting the symmetry of the crystal lattice. Thus, the next step of the work would be to investigate the elastic properties of C-S-H crystal in the two other directions.

References

[1] A. Boumiz, C. Vernet, F. Cohen Tenoudji, Mechanical properties of cement pastes and mortars at early ages, Advanced Cement Based Materials 3 (1996) 94-106

[2] F.H. Heukamp, F.J. Ulm, J.T. Germaine, poroplastic properties of calcium-leached cement-based materials, Cem Concr Res 33 (2003) 1155-1173

[3] K. Velez, S. Maximilien, D. Damidot, G. Fantozzi, F. Sorrentino, Determination by nanoindentation of elastic modulus and hardness of pure constituents of Portland cement clinker, Cem Concr Res 31 (2001) 555-561

[4] D. Damidot, K. Velez, F. Sorrentino, Characterization of interstitial transition zone (ITZ) of high performance cement by nanoindentation technique, Proceeding of the 11th ICCC, Durban, South Africa, (2003) 314-323

[5] J.J. Hugues, P. Trtik, Micro-mechanical properties of cement paste measured by depth-sensing nanoindentation: a preliminary correlation of physical properties with phase type, Materials Characterization 53 (2004) 223-231

[6] F.H. Wittmann, Estimation of the modulus of elasticity of calcium hydroxide, Cem Concr Res 16 (1986) 971-972

[7] J.J. Beaudoin, Comparison of mechanical properties of compacted calcium hydroxide and Portland cement paste systems, Cem Concr Res 13 (1983) 319-324

[8] O. Bernard, F.J. Ulm, E. Lemarchand, A multiscale micromechanics-hydration model for the early-age elastic properties of cement-based materials, Cem Concr Res 33 (2003) 1293-1309

[9] C.J. Haecker, E.J. Garboczi, J.W. Bullard, R.B. Bohn, Z. Sun, S.P. Shah, T. Voigt, Modeling the linear elastic properties of Portland cement paste, Cem Concr Res 35 (2005) 1948-1960

[10] S.P. Baker, Between nanoindentation and scanning force microscopy: measuring mechanical properties in the nanometer regime, Thin Solid Films 308-309 (1997) 289-296

[11] S. Chowdury, M.T. Laugier, I.Z. Rahman, Measurement of the mechanical properties of carbon nitride thin films from the nanoindentation loading curve, Diamond and Related Materials 13 (2004) 1543-1548

[12] S. Chowdury, E. de Barra, M.T. Laugier, Study of mechanical properties of CVD diamond on SiC substrates, Diamond and Related Materials 13 (2004) 1625-1631

[13] B.K. Jang, H. Matsubara, Hardness and Young's modulus of nanoporous EB-PVD YSZ coatings by nanoindentation, Journal of Alloys and Compounds 402 (2005) 237-241

[14] B.K. Jang, H. Matsubara, Influence of porosity on hardness and Young's modulus of nanoporous EB-PVD TBCs by nanoindentation, Materials Letters 59 (2005) 3462-3466

[15] Z.M. Sun, A. Murugaiah, T. Zhen, A. Zhou, M.W. Barsoum, Microstructure and mechanical properties of porous Ti_3SiC_2, Acta Materialia 53 (2005) 4359-4366

[16] G. Constantinides, F.J. Ulm, The effect of two types of C-S-H on the elasticity of cement-based materials: results from nanoindentation and micromechanical modeling, Cem Concr Res 34 (2004) 67-80

[17] X. Chen, Novel technique for measuring the mechanical properties of porous materials by nanoindentation, J Mater Res 21 (2006) 715-724

[18] T.C. Powers, Properties of cement Portland concrete, Proceedings of the 4th ICCC, Washington (1960) 571-609

[19] R.E. Williford *et al*, Mechanical stability of templates mesoporous silica thin films, Microporous and Mesoporous Materials 85 (2005) 260-266

[20] S. Sundararajan, B. Bushan, Development of AFM-based techniques to measure mechanical properties of nanoscale structures, Sensors and Actuators A 101 (3) (2002) 338-351

[21] B. Bushan, Nano to microscale wear and mechanical characterization using scanning probe microscopy, Wear 251 (2001) 1105-1123

[22] M. Finke, J.A. Hugues, D.M. Parker, K.D. Jandt, Mechanical properties of in situ demineralised human enamel measured by AFM nanoindentation, Surf Sci 491 (3) (2001) 456-467

[23] E. Finot, E. Lesniewska, J.C Mutin, J.P Goudonnet, Investigations of surface forces between gypsum crystals in electrolytic solutions using microcantilevers,J Chem Phys 111 (14) (1999) 6590-6598

[24] E. Finot, E. Lesniewska, J.P Goudonnet, J.C Mutin, Correlation between surface forces and surface reactivity in the setting of plaster by AFM, Appl Surf Sci 161 (3-4) (2000) 316-322

[25] E. Finot, E. Lesniewska, J.P Goudonnet, J.C Mutin, M. Domenech, A. Aït Kadi, Correlating surface forces with surface reactivity of gypsum crystals by AFM. Comparison with rheological properties of plaster, Solid State Ionics 141-142 (2001) 39-46

[26] S. Lesko, E. Lesniewska, A. Nonat, J.C. Mutin, J.P. Goudonnet, Investigation by atomic force microscopy of forces at the origin of cement cohesion, Ultramicroscopy 86 (2001) 11-21

[27] C Plassard, E. Lesniewska, I. Pochard, A. Nonat, Investigation of the surface structure and elastic properties of calcium silicate hydrates at the nanoscale, Ultramicroscopy 100 (2004) 331-338

[28] S. Gauffinet, E. Finot, A. Nonat, Experimental study and simulation of C-S-H nucleation and growth, Proceedings of the 2nd. International RILEM workshop on hydration and setting, RILEM Publications (1997) 199-214

[29] S. Gauffinet, E. Finot, E. Lesniewska, A. Nonat, Direct observation of growth of C-S-H on alite and silica surfaces by AFM, Comptes Rendus de l'Academie des Sciences Paris 327 (4) (1998) 231-236

[30] C-C. Chen, C-C. Lin, L-G. Liu, S.V. Sinogeikin, J.D. Bass, Elasticity of single-crystal calcite and rhodochrosite by Brillouin spectroscopy, Am. Mineral. 86 (2001) 1525-1529

[31] K.L. Johnson, K. Kendall, A.D. Roberts, Surface energy and the contact of elastic solids, Proc. R. Soc. A 324 (1971) 301-313

[32] J.A. Gard, H.F.W. Taylor, The crystal structure of foshagite, Acta Crystallogr. 13 (1960) 785-793

[33] J.L. Laugensen, Copenhagen University, Denmark, unpublished results

[34] S. Habelitz, G.Carl, C.Rüssel, S. Thiel, U. Gerth, J.D. Schnapp, A. Jordanov, H. Knake, Mechanical properties of oriented mica glass ceramic, Journal of Non-Crystalline Solids 220 (2,3) (1997) 291-298

[35] I. Klur, B. Pollet, J. Virlet, A. Nonat, C-S-H structure evolution with calcium content by mulitnuclear NMR, Proceeding of NMR spectroscopy of cement-based materials, Bergamo, Italy (1998) 119-141

[36] A. Gmira, M. Zabat, R.J.M. Pellenq, H. van Damme, Microscopic physical basis of the poromechanical behavior of cement-based materials, Materials and Structures 37 (265) (2004) 3-14

[37] R. Astala, M. Kaukonen, R.M. Nieminen, Nanoindentation of silicon surfaces: molecular-dynamics simulations of atomic force microscopy, Physical Review B 61 (2000) 2973-2980

[38] P. Acker, Micromechanical analysis of creep and shrinkage mechanisms, Creep, Shrinkage and Durability Mechanics of Concrete and other Quasi-Brittle Materials, edited by ULM F.J., BAZANT Z.P. and WITTMANN F.H, 2001

[39] P. Acker, F.J. Ulm, Creep and shrinkage of concrete: physical origins and practical measurements, Nuclear Engineering and Design 203 (2001) 143-158

[40] F.J. Ulm, Chemomechanics of concrete at finer scales, Materials and Structures 36 (2003) 426-438

[41] F.J. Ulm, G. Constantinides, F.H. Heukamp, Is concrete a poromechanics material? a multiscale investigation of poroelastic properties, Materials and Structures 37 (2004) 43-58

[42] P.D. Tennis, H.M. Jennings, A model for two types of calcium silicate hydrate in the microstructure of Portland cement pastes, Cem Concr Res 30 (2000) 855-863

[43] H.M. Jennings, A model for the microstructure of calcium silicate hydrate in cement paste, Cem Concr Res 30 (2000) 101-116

[44] J.J. Beaudoin, R.F. Feldman, J. Baron, M. Conjeaud, Dependence of degree of silica polymerization and intrinsic mechanical properties of C-S-H on Ca/Si ratio, Proceeding of the 8th Congr. Int. Quim. Cimento (1986) 337-342

[45] M. Grutzeck, A. Benesi, B. Fanning, Silicon-29 magic angle spinning NMR study of C-S-H, Journal of the American Ceramic Society 72 (4) (1989) 665-668

[46] A. Nonat, X. Lecoq, The structure, stoechiometry and properties of C-S-H prepared by C_3S hydration under controlled condition, Proceeding of

NMR spectroscopy of cement-based materials, Bergamo, Italy (1998) 197-207